JOURNAL OF MATERIALS SCIENCE 13 (1978) 1611–1631

Review
Ostwald ripening and its application to precipitates and colloids in ionic crystals and glasses

S. C. JAIN*, A. E. HUGHES
Materials Development Division, Atomic Energy Research Establishment, Harwell, Didcot, Oxon, UK

The theory of Ostwald ripening developed by Lifshitz and Slezov and by Wagner (LSW theory) has been used for many years to interpret ageing experiments in metallic alloys. The theory is reviewed, and extended in some respects which are suggested by using it to interpret experiments on the ripening of precipitates and colloids in non-metallic systems. A detailed treatment is given for the case where the diffusion of solute species down dislocations or grain boundaries controls the ripening rate and the particle size distribution. The assumptions and approximations used in the theory are examined, and it is shown that an inhomogeneous spatial distribution of particles can lead to several independently ripening systems within the same sample if groups of particles are separated by distances large compared with the interparticle separation within each group. The theory is then used to interpret observed size distributions of precipitates in alkali halides and glass. Some of the data do not fit into the framework of the LSW theory and it is suggested that this is the result of the extremely inhomogeneous spatial distributions of particles found in electron microscope studies of these systems

1. Introduction

Studies of the precipitation of particles from a supersaturation of a solute in a crystal matrix were first made by Frank, [1], Zener [2], Wert [3], Wert and Zener [4, 5], Ham [6, 7] and others (see Christian [8] for references to other papers). If the time of nucleation is relatively short, the particle size distribution remains narrow during the process of precipitation from a high supersaturation. However, when most of the excess solute has been precipitated, and the supersaturation has become small, the smaller particles begin to dissolve and the larger particles grow by "devouring" the smaller particles, a process known as Ostwald ripening. The driving force for Ostwald ripening arises because the concentration of solute in the vicinity of small particles is greater, and that in the vicinity of large particles less, than the average supersaturation. The solute therefore flows from small particles to the crystal matrix and from the matrix to the large particles. The theory of Ostwald ripening was formulated by Greenwood [9] and considerably extended by Lifshitz and Slezov [10–12] and Wagner [13], and has become known as LSW theory. Modifications to the theory have been suggested by Ardell [14], Dunning [15] and Kahlweit [16–18]. The LSW theory predicts that for large values of time, the average radius $\bar{R}$ grows as t^n where $n < 1$ and the size distribution expressed as $F(R/\bar{R})$ does not depend on time. A number of reviews of Ostwald ripening theory have been published (for example [17, 19, 20]), treating various aspects of the problem.

*Permanent address: Defence Research and Development Organisation, South Block, New Delhi-11, India.

Extensive experimental work has been done on the measurement of size distributions of precipitates in metal alloys (see the review by Greenwood [20]), notably by Ardell and associates (see [21] for reference to several earlier papers). In the majority of cases studied, the average particle radius $\bar{R}$ seems to follow the $t^{1/3}$ growth law, as predicted by the theory when the ripening process is controlled by volume diffusion of solute through the matrix*. However, in most cases, the observed size distribution curves are much wider than those predicted by the theory. In many cases, a few large particles are found, which do not form part of the main system of particles. In some cases, a tail on the large size side is observed, in complete contradiction to the LSW theory, which predicts distributions with a sharp cut-off.

More recently, size distributions of colloids and precipitates in non-metals have been reported [24–30], and attempts have been made to interpret some of the results theoretically [31, 32]. Except for the results for silver particles in KCl [26], where the size distributions are narrow, the observed distributions have the same general features as precipitates in metal alloys discussed above. The K and Na colloid size distributions in KCl and NaCl [24] have a tail on the large size side. The size distribution of silver particles in photosensitive glass observed by Kreibig [25] is too wide, and a few large particles, which do not form part of the general system of particles, are observed. In NaCl crystals containing a low Mn concentration, the size distribution of $MnCl_2$: 6NaCl precipitates (Suzuki phase) [27] appears to be similar to the distributions observed in metal alloys. As the concentration of Mn increases, the distribution becomes very complex. In view of all these deviations between experiment and the LSW theory, it seems pertinent to examine the limitations of the theory and the extent to which modifications which take further account of the physics of the problem can improve the understanding of Ostwald ripening processes, particularly in non-metallic systems.

The effect of dislocations or grain boundaries on transport of solute atoms is well known [7, 20, 28–30, 33–38]. It is not clear whether any of the discrepancies discussed above could be due to the effect of dislocation diffusion on the size distribution, since the detailed statistical theory for this case has not previously been fully developed [20]. In the next section we extend the LSW theory to the case of dislocation or grain boundary diffusion, making the same approximations as used by Lifshitz, Slezov and Wagner. In Section 3 we examine critically some of the approximations used in the theory. Using the results obtained in Sections 2 and 3, we compare, in Sections 4 and 5, the size distributions observed in non-metals with the modified theories. The results point to some new features of Ostwald ripening which are of general interest in materials science.

2. Ripening theory and its extension to the case of diffusion through dislocations or grain boundaries

2.1. The three basic cases

During Ostwald ripening, solute atoms must diffuse through the matrix so that matter can be transported from small precipitates to large precipitates. This implies that solute atoms can evaporate freely from the small particles and then condense on the large particles once they have arrived in their vicinity. Although in principle the theory can be developed for the general case where both processes are considered [13, 20], analytical results are only obtained when one of these steps is the rate-limiting process. We can distinguish three different cases, according to the transport or reaction process which is considered to determine the kinetics of the particle ripening. If evaporation or condensation of solute at the precipitates is the rate-controlling process, regardless of the mechanism of diffusion through the matrix, then we have what is referred to as the "surface reaction" case, case 1. Case 2 refers to the situation where the rate-controlling step is bulk diffusion of solute through the matrix, the "volume diffusion" case. Finally, case 3 covers the situation where diffusion of solute through the matrix takes place by dislocation pipe or grain boundary diffusion. Simple theoretical results can be obtained if any one of these three processes determines the rate of ripening. The LSW theoretical results for the first two cases are available (see [20]). We derive the results for the dislocation or grain boundary case in this section. Some other cases (e.g. surface reaction limited with second-order

*See however Smith [22] who showed that the same experimental data can be fitted with $t^{1/3}$ and $t^{1/2}$ laws, the latter being valid for the case where the ripening rate is controlled by surface reactions at the precipitate. (See also discussion after the paper by Mukherjee and Sellars [23]).

kinetics) have been discussed by Kahlweit [17, 19].

The assumptions under which we shall develop the theory are the same as those discussed by Wert and Zener [5] and Greenwood [9], and used by Lifshitz and Slezov [10] and Wagner [13]. We shall discuss some of these assumptions in Section 3 after presenting the main results. To make the article self-contained, the detailed mathematical steps are included as appendices.

2.2. Growth rate of particle radius, dR/dt

In Ostwald ripening, the large particles or precipitates grow and the small ones shrink. The solute atoms migrate to the growing particles and away from the shrinking particles. For convenience, we shall generally discuss the "growing" particles and the "migration to" the particles. The case of shrinking particles follows by implication. Both cases will be discussed explicitly where necessary.

In general the particle will receive solute directly from the matrix by bulk diffusion as well as by diffusion through dislocations or grain boundaries. If the dislocation density is large and if the temperature is not high, the amount of solute received through dislocations or subboundaries (or grain boundaries in the case of polycrystals) can be considerably greater than that received by bulk diffusion. We first discuss the case of dislocation diffusion. The meaning of all the symbols used is summarized in Appendix 1. The calculation is considered in more detail in Appendix 2.

Consider a precipitate particle connected to the solute in the matrix through a dislocation line of "radius" a (Fig. 1a)*. The diffusion equation for transport of solute within the dislocation line is (in the steady state approximation where $\dot{C} = 0$, see Section 3.3)

$$\pi a^2 D_1 \frac{d^2 C}{dx^2} + j(x) = 0 \qquad (1)$$

where $j(x)$ is the total flux of solute atoms entering the dislocation line from the bulk at a distance x from the precipitate.

The boundary conditions along the dislocation line are

$$C(x) = C_R \text{ when } x = R \qquad (2)$$

and

$$C(x) = C_a \text{ when } x \to \infty \qquad (3)$$

Consider now the solute concentration outside the dislocation line. Except very near the particle, the concentration is practically uniform everywhere in the absence of the dislocation line. However, in the presence of the dislocation line, the concentration near the dislocation line i.e. for $s \gtrsim a$ (Fig. 1a) will change, but will attain its average value C_a at large values of s. The problem of calculating $j(x)$ thus reduces to that of radial diffusion into an infinite cylinder with the boundary conditions

$$C = C(x) \text{ when } s = a \qquad (4)$$

$$C = C_a \text{ when } s \to \infty \qquad (5)$$

The solution of radial flow in an infinite cylinder is well known [40] and we can easily calculate $j(x)$, integrate Equation 1 and obtain an expression for

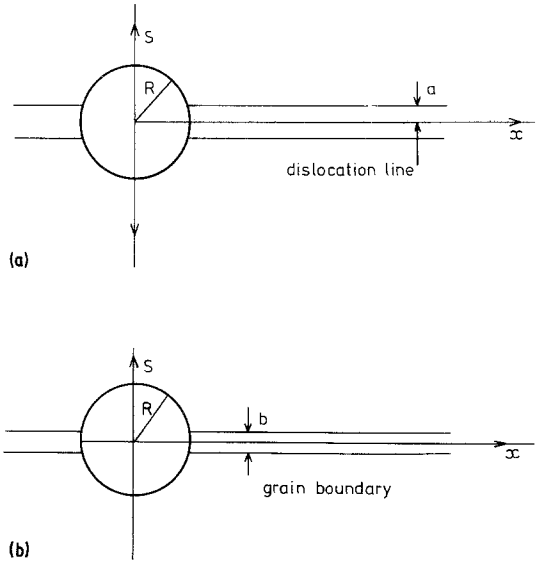

Figure 1 A spherical particle ripening (a) on a dislocation line, and (b) on a grain boundary.

*The stress field of the dislocation line causes the atoms to drift into the dislocation line [39]. For the large values of time ($t = 0$ when precipitation begins) with which we are concerned in the ripening process, the drift is taken into account by replacing a by an effective capture radius a_e [7, 36] given by

$$a_e = mB/kT \qquad (6)$$

where B is the strength of the dislocation potential and $m = 1.80$ for the screw dislocation and 0.45 for the edge dislocation.

the solute current density $D_1 (dC/dx)_{x=R}$ into the particle (see Appendix 2). The conservation of solute atoms then leads to an equation for the rate of change of particle radius.

$$(C_p - C_R)\, 4\pi R^2 \frac{dR}{dt} = 2\pi a^2 D_1 \left(\frac{dC}{dx}\right)_{x=R} \tag{7}$$

With $C_p \gg C_R$ this leads to an expression for dR/dt of the form

$$\frac{dR}{dt} = \frac{G}{R^2} \frac{(C_a - C_R)}{C_p} \tag{8}$$

where G is a constant which involves the diffusion coefficients D_1 and D and can easily be evaluated (see Appendix 2).

Bullough and Newman [36] have used a "gas like" boundary condition instead of Equation 4 in order to calculate the flow of solute atoms into the dislocation line. It is shown in Appendix 2 that their treatment also leads to an expression of the same type as Equation 8. It is clear that $\dot{R} \propto R^{-2}$ will result from any model where the solute current to the particle is independent of R.

We now discuss the case of grain boundary diffusion. Appendix 2 describes in detail our extension and generalization of the treatment given by Chakraverty [41], Vengrenovitch and Psarev [42] and Vengrenovitch [43] for particles on a surface, and by Speight [34] and Greenwood [20] for particles at grain boundaries. The diffusion equation for diffusion through the grain boundary is

$$\frac{D_g b}{x} \frac{\partial}{\partial x} \frac{x \partial C}{\partial x} + j'(x) = 0 \tag{9}$$

where $j'(x)$ takes account of the flux of solute from the bulk to the grain boundary surface. The boundary conditions are

$$C = C_R \text{ at } x = R \tag{10}$$

$$C = C_a \text{ at } x = L, L \gg R \tag{11}$$

The solute current $j'(x)$ can be calculated assuming steady state diffusion from the matrix into the grain boundary (as was done in the case of bulk diffusion by Lifshitz and Slezov [12] and Wagner [13]), and using the boundary condition that $C = C_a$ at some large distance l from the boundary. Equation 9 can then be integrated in terms of Bessel functions of the second kind (see Appendix 2). Using approximations $D_g/D \gg R^2/lb$, $C_p \gg C_R$ and that $\ln (4 D_g lb/DR^2)$ is a slowly varying function of R, the solution can be shown to reduce to the form in Equation 8.

2.3. Ripening rate and size distribution for the grain boundary or dislocation case

The size distribution $f(R, t)$ is obtained by the solution of the continuity equation [10, 13]

$$\frac{\partial f}{\partial t} = -\frac{\partial (f.\dot{R})}{\partial R} \tag{12}$$

under conditions where the total number of solute atoms is conserved and $\dot{R} = dR/dt$ is given by an equation such as Equation 8. We follow the method of Lifshitz and Slezov in order to find the distribution function $f(R, t)$ for the quasi-steady state reached at large values of t.* The procedure is described in detail in Appendix 3, and we confine ourselves in this section to the main results of this treatment for case 3 and compare them with the results of cases 1 and 2 (see Section 2.1) as derived by Lifshitz and Slezov [10, 12], Wagner [13] and others.

The starting point in all treatments is to express the concentration of solute C_R in equilibrium with the particle of radius R by Thomson's equation (see for example [9]).

$$C_R = C_\infty \exp(\alpha/R) \tag{13a}$$

where C_∞ is the solute concentration in equilibrium with a plane surface and $\alpha = 2\Omega\sigma/kT$ where Ω is the atomic volume and σ the interfacial energy of the particle in the matrix. (Note that Lifshitz and Slezov use a different definition of α, and C_p seems to be omitted from the expressions in their papers).

Assuming $\alpha \ll R$ (see Section 3 for a discussion of this point), Equation 13a can be expanded to give

$$C_R = C_\infty (1 + \alpha/R) \tag{13b}$$

*This asymptotic region of the LSW theory cannot persist to *very* large times, because ultimately the system should ripen into one large particle. This point is discussed in papers by Kahlweit [16–18], but he does not derive any analytical expression for the upper limit of time. This is an aspect of the theory where numerical calculations may be helpful in the future. In this review we confine attention to the LSW region.

which allows Equation 8 to be written as

$$\frac{dR}{dt} = \frac{G\alpha C_\infty}{C_p R^2}\left(\frac{1}{R_c} - \frac{1}{R}\right) \tag{14}$$

Here R_c, the "critical radius", is the radius of a particle which is *instantaneously* in equilibrium with the mean solute concentration so that $C_R = C_a$ and $\dot{R} = 0$. From Equation 13b,

$$C_a = C_\infty(1 + \alpha/R_c). \tag{15}$$

R_c is a crucial parameter in the LSW theory, since the radius distribution function expressed in terms of the reduced variable R/R_c is found to be asymptotically independent of the time t.

Following the method of Lifshitz and Slezov, we use the following substitutions (see Appendix 3)

$$u = R/R_c \tag{16}$$

$$\tau = \ln \frac{R_c^4(t)}{R_c^4(0)} \tag{17}$$

Equation 14 can now be expressed as

$$\frac{du^4}{d\tau} = \gamma(u-1) - u^4 \tag{18}$$

where

$$\gamma = \frac{4\alpha G C_\infty}{C_p}\frac{dt}{d(R_c^4)} \tag{19}$$

Lifshitz and Slezov present rather involved arguments to show that γ must tend to a constant γ_0 for large values of time. Precisely the same arguments can be used in our case, and lead to the same conclusion. The value of γ_0 is found by demanding that $du/d\tau$ and its first derivative with respect to u are zero at some value of $u = u_0$. Following this procedure, we get

$$\gamma_0 = 4u_0^3 \tag{20}$$

and

$$u_0 = 4/3 \tag{21}$$

We now follow further the method of Lifshitz and Slezov and integrate Equation 12 with the help of Equations 18 to 21, see Appendix 3. The final results can be put in the form, valid for large times (such that $R_c \gg R_c(0)$, see [12]):

$$f(R, t) = \frac{\text{Constant}}{t} F_3(u) \tag{22a}$$

$$F_3(u) = \frac{u^3 \exp\left[\frac{-2}{3(u_0-u)}\right]\exp\left[-\frac{1}{6\sqrt{2}}\tan^{-1}\left(\frac{u+u_0}{u_0\sqrt{2}}\right)\right]}{(u_0-u)^{19/6}(u^2+2u_0u+4u_0)^{23/12}}$$

for $u \leqslant 4/3$, and $F_3(u) = 0$ for $u > 4/3$. (22b)

For $t \gg \tau_3 = \dfrac{64 C_p R_c^4(0)}{27\alpha G C_\infty}$:

$$R_c^4 = R_c^4(0)(1 + t/\tau_3) \tag{23}$$

$$C_a - C_\infty = \frac{\alpha C_\infty}{R_c} \propto t^{-1/4} \tag{24}$$

$$n(t) \propto t^{-3/4} \tag{25}$$

For the sake of completeness we write below corresponding expressions for the surface reaction and the bulk diffusion cases and show the plots of $F_1(u)$, $F_2(u)$ and $F_3(u)$ in Fig. 2.

For case 1 i.e. for surface reaction controlled ripening, we have

$$F_1(u) = u\frac{\exp[-3u/(2-u)]}{(2-u)^5} \text{ for } u \leqslant 2.0,$$

$$F_1(u) = 0 \text{ for } u > 2.0 \tag{26}$$

For $t \gg \tau_1 = \dfrac{2 C_p R_c^2(0)}{\alpha K C_\infty}$:

$$R_c^2 = R_c^2(0)(1 + t/\tau_1) \tag{27}$$

$$C_a - C_\infty \propto t^{-1/2} \tag{28}$$

$$n(t) \propto t^{-3/2} \tag{29}$$

Similarly for the bulk diffusion case, case 2, we have

$$F_2(u) = u^2\frac{\exp[-2u/(3-2u)]}{(3+u)^{7/3}(3-2u)^{11/3}} \text{ for } u \leqslant 1.5,$$

$$F_2(u) = 0 \text{ for } u > 1.5. \tag{30}$$

For $t \gg \tau_2 = \dfrac{9 C_p R_c^3(0)}{4\alpha D C_\infty}$:

$$R_c^3 = R_c^3(0)(1 + t/\tau_2) \tag{31}$$

$$C_a - C_\infty \propto t^{-1/3} \tag{32}$$

$$n(t) \propto t^{-1} \tag{33}$$

In all cases

$$R_c = f\bar{R} \tag{34}$$

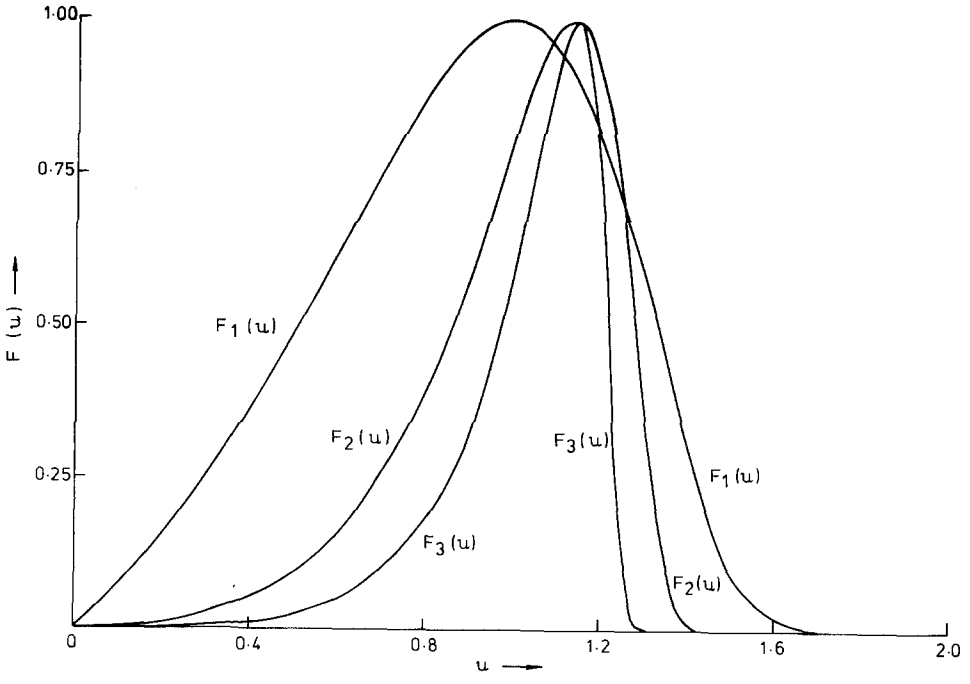

Figure 2 Theoretical size distributions: $F_1(u)$ for the surface reaction case, $F_2(u)$ for the bulk diffusion case and $F_3(u)$ for the dislocation and grain boundary diffusion case. The maximum values of the three functions occur at $u = 1.00$, $u = 1.135$ and $u = 1.142$ and the functions become zero at $u = 2.00$, $u = 1.50$ and $u = 1.33$ respectively. Note that $F(u)$ varies as u, u^2 and u^3 near $u = 0$ in the three cases, and the distribution becomes sharper in going from the surface reaction case to the bulk diffusion case and from the bulk diffusion case to the dislocation and grain boundary diffusion case. The critical radius R_c grows at $t^{1/2}$, $t^{1/3}$ and $t^{1/4}$ respectively in the three cases.

where $f = 1$ for the bulk diffusion case and is close to 1 for the other cases. In fact, in all cases it is possible to relate R_c exactly to the mean value of some power of the radius (see Appendix 3 and [13]). Thus in case 3 we find $R_c^{-1} = R^{-1}$.

2.4. Comparison of the three cases

If we write

$$\frac{dR}{dt} = \frac{\text{constant}}{R^n}\left(\frac{1}{R_c} - \frac{1}{R}\right) \tag{35}$$

then $n = 0$, 1 and 2 respectively for the three cases discussed above (see [20]). The maximum of dR/dt occurs at values of R given by

$$R = \frac{n+1}{n} R_c \tag{36}$$

There is no value of R for which dR/dt is a true maximum for the surface reaction case for which $n = 0$. For the bulk diffusion case ($n = 1$) and the dislocation diffusion case ($n = 2$), the maxima of dR/dt occur at $R/R_c = u = 2$ and 3/2 respectively. It is tempting to argue that since particles of these radii grow at a maximum rate, the maxima of the size distributions may occur near these values. The size distribution expressions show that particles of these radii are never present once the asymptotic limit is reached, and in fact maxima in the three cases occur (Fig. 2) at $u = 1.000$, 1.135 and 1.142 i.e. increasing with n, a trend opposite to that of the values at which maxima of dR/dt occur. As the value of n increases, the dependence of dR/dt and $F(R/R_c)$ on R becomes stronger. For $u = R/R_c \to 0$, the $1/R_c$ term in Equation 35 can be neglected and dR/dt varies as $1/R^{n+1}$ and $F(R/R_0)$ as $(R/R_c)^{n+1}$. Thus near $u = 0$, $F(u)$ rises as u, u^2 and u^3 respectively in the three cases (Fig. 2). Near the peak of $F(u)$, the behaviour is largely controlled by $\left(\frac{1}{R} - \frac{1}{R_c}\right)$. For $R > R_c$, the large particles are not able to grow so quickly for large values of n, giving a sharper cut-off for the dislocation/grain boundary case than for the others, as can be seen in Fig. 2.

3. Approximations involved in the theory

3.1. Details of precipitate shapes and solute diffusion mechanisms

Although the ripening theory was developed for highly idealized conditions, in many cases the main results of the theory can be used even if the conditions are not so ideal. Lifshitz and Slezov [11, 12] have shown that the results of the theory can be used even if the precipitate particles are not spherical and even if lattice anisotropy and strains are present, provided the parameters in the theory (such as radius of the particle R and diffusion coefficient D) are reinterpreted and modified. Wagner [13] discussed the modification necessary in the Thomson equation (Equation 13) if the solute consists of dissociating molecules. The growth of a precipitate involves not only transport of solute atoms (or molecules) from solute rich regions to the neighbourhood of the precipitate, but also transport of the host lattice atoms from the neighbourhood of the precipitate to distant regions. The mechanisms of volume tansfer have been considered by Oriani [44]. Oriani showed how the parameter D used in the theory should be reinterpreted or modified for the different mechanisms of volume transport. Li *et al.* [45] have also considered how D should be interpreted for multi-component diffusion.

These modifications leave the main results (growth law for the critical radius R_c and expressions for the distribution of sizes etc.) unaltered. They become important only if we use the results to derive values of σ, the surface energy, or D, the diffusion coefficient, and therefore make ripening rates a dubious method for determining these parameters. The modifications cannot be invoked to explain the discrepancy between theory and experiment discussed in the Introduction, since these involved the size distribution functions.

We discuss below some other approximations used in the theory and their effects on the final results.

3.2. Thomson's equation – the capillarity effect

For large values of R, both Equations 13a and b are valid. However, for $\alpha/R \gtrsim 0.3$, the approximation in Equation 13b becomes poor. Wagner has argued that the error involved is not significant since the population of the small particles is relatively very small. Though this statement may be true for the growth of R_c and hence $\bar{R}$, the error can still have a significant effect on the shape of $F(u)$, particularly for small values of u. To see this, we may proceed as follows.

The total number of particles per unit volume $n(t)$ is given by

$$n(t) = \int_0^\infty f(R, t)\,dR \tag{37}$$

and from Equation 12 it follows that (see [13])

$$-\frac{dn}{dt} = -\frac{d}{dt}\int_0^\infty f(R, t)dR = -\lim_{R\to 0}[f(R, t)\dot{R}].$$

Since dn/dt must depend only on t, it follows that as $R \to 0$ the function $f(R, t)$ must show the inverse functional dependence on R to $\dot{R}$. This enables us to find the limiting form of $f(R, t)$ without approximating Thomson's equation.

In general dR/dt in the three cases has the form

$$\frac{dR}{dt} = \frac{\text{constant}}{R^n}(C_a - C_R) \tag{39}$$

which leads to Equation 35 when Thomson's equation is approximated by Equation 13b. However, if we use instead Equation 13a, then we have

$$\frac{dR}{dt} \simeq \frac{\text{constant}}{R^n} C_\infty e^{\alpha/R_c}\,[1 - e^{\alpha(1/R - 1/R_c)}] \tag{40}$$

Thus it is clear that, as $R \to 0$

$$f(R, t) \propto \frac{R^n}{e^{\alpha/R} - 1} \simeq R^n e^{-\alpha/R} \tag{41}$$

This is to be contrasted with $f(R, t) \propto R^{n+1}$ which results when Equation 13b is used.

Equation 41 shows that the effect of including the proper form of Thomson's equation suppresses the population of very small partilces. We can understand this result from general physical considerations. For small particles the actual value of C_R is larger than that given by Equation 13b, the solute currents are stronger and dissolution rates higher than those calculated on the basis of Equation 13b. A comparison of Equation 41 and R^{n+1} is shown in Fig. 3. It can be seen that the changes in $f(R, t)$ at small R are most obvious for case 1.

The values of interfacial energy σ are not known with any certainty for most systems (see Scott [46] for colloids in alkali halides and

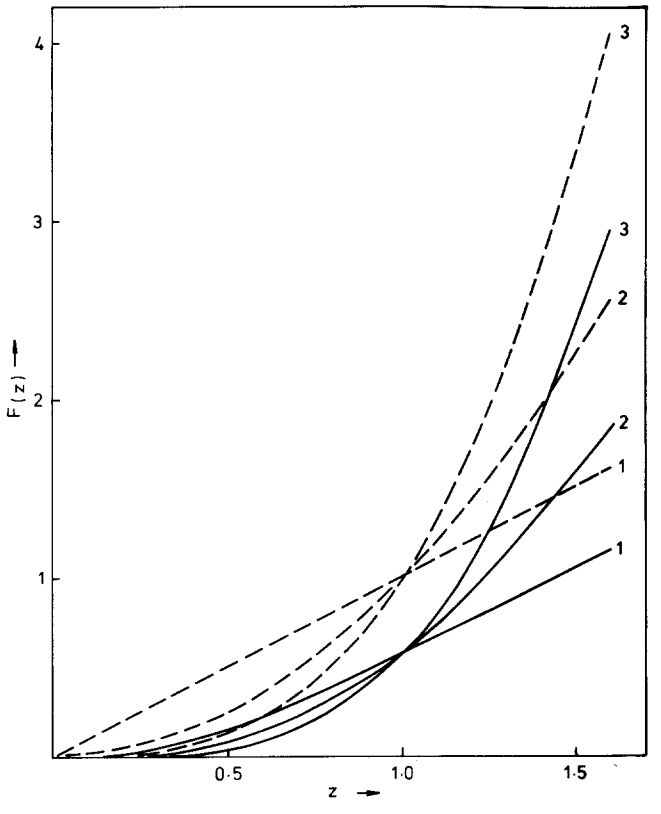

Figure 3 Comparison of the functions $F(z) = z^n/(e^{1/z} - 1)$(full lines) and $F(z) = z^{n+1}$ (dashed lines) for $n = 0$, 1 and 2 as appropriate for cases 1, 2 and 3. The variable z is written for R/α (see text).

Oriani [44] for precipitates in metal alloys). Taking a probably high value of $\sigma = 1000$ ergs cm^{-2}, $\Omega \simeq 5 \times 10^{-23}$ cm^3 and $T = 1000$ K gives $\alpha \simeq 7$ nm and the discrepancy due to the approximation in Equation 13b will become significant for $R \gtrsim 20$ nm. Smaller values of σ improve the situation so that for $\sigma \sim 10$ ergs cm^{-2} (typical of Ni_3Al in Ni) the approximation is very good.

Recent theoretical work [47, 48] suggests that the binding energy decreases with size for very small particles (containing $\gtrsim 20$ atoms); the interfacial energy also becomes size dependent. Equation 13a itself will not then remain valid for such small particles and will underestimate C_R (see also [9]). Presumably these effects will accelerate the disintegration rates and reduce further the population of the very small particles.

Since the value of $C_a(t)$ will be affected by the higher dissolution rates of these small particles, other parts of the distribution curve (i.e. for large values of R) may also change. However, it seems clear from the preceding arguments that the major effect of the approximations in Equations 13a and b will be to change the functional dependence of $f(R, t)$ on R as $R \to 0$.

3.3. Steady state diffusion and homogeneous distribution approximations

To obtain expressions for dR/dt in cases 2 and 3 where diffusion is involved, it is necessary to calculate the solute currents to a growing particle or from a shrinking particle. This involves solving the diffusion equation

$$D\nabla^2 C = \partial C/\partial t \qquad (42)$$

under the following usual assumptions.

(1) The interparticle distance λ (or distance λ_1 between two dislocations) is much larger than the radius R of the particle (or the effective capture radius a_e in the case of dislocations, case 3).

(2) The distribution of particles (or dislocations) is uniform to satisfy (1) and to permit the approximation of spherical symmetry in case 2 and cylindrical symmetry in case 3.

(3) The concentration C is described by steady state diffusion, i.e. $\partial C/\partial t$ and dR/dt are assumed to be zero while calculating C as a function of distance from the particle (see also Appendix 2).

These are the assumptions also used by Wert and Zener [5] in their treatment of precipitation.

The first term of the more complete eigenvalue series of Ham [6] is exactly equivalent to the treatment of Wert and Zener, for the spherical particle in case 2, and dominates the kinetics when $\lambda \gg R$. It can also be shown [49] that steady state diffusion conditions are satisfied very well when $C_p/(C_a - C_R) \gg 1$, which holds well during the ripening process. The critical assumptions are, therefore, the assumptions (1) and (2) above.

We discuss the first two approximations, in particular the effect of deviations from uniform distribution, for case 2. The arguments can be easily extended to the other two cases, if necessary, with similar conclusions.

3.4. Inhomogeneities in the Frank–Zener precipitation regime

We first consider the growth of particles from high supersaturation studied by Zener [2] and Frank [1] and then extend the argument to the ripening case.

In the case of precipitation and growth of particles of equal radius R (as distinguished from Ostwald ripening, designated as the LSW regime), the characteristic time τ_z for the depletion of supersaturation $C_a - C_R$ is given [5]

$$\tau_z = \lambda^3/DR \tag{43}$$

where λ is the mean interparticle separation. The distance over which any fluctuation in C_a will be smoothed out in this time is $\lambda(\lambda/R)^{1/2}$. Any deviations from an ideally random distribution will therefore not affect significantly the kinetics of the precipitation process if they are limited to distances of this order. For $\lambda \sim 10R$ this limiting distance is a few λ. However, it is clear that any variation in C_a over a distance larger than this will not be able to come into equilibrium during the precipitation process, and that the kinetics of precipitation must then be altered.

Now consider two regions of the crystal separated by a distance L. Let the particles be ideally distributed (i.e. fluctuation confined to distances $<$ few λ) in each region, but suppose that the values of λ and R (or of either one of them) are different in the two regions, say λ_1 and R_1 in the first region and λ_2 and R_2 in the second region respectively. The two regions will behave almost independently and the values of R as well as $C_a(t)$ will continue to be different in the two regions if the time τ_1 needed for smoothing out the difference in $C_a(t)$, given by

$$\tau_1 = L^2/D \tag{44}$$

is much larger than

$$\tau_z \sim \frac{\lambda_1^3}{R_1 D} \sim \frac{\lambda_2^3}{R_2 D}$$

i.e. if

$$L/\lambda_{1,2} \gg (\lambda/R)_{1,2}^{1/2} \sim 3 \text{ for } (\lambda/R)_{1,2} \sim 10 \tag{45}$$

The difference in $C_a(t)$ or R between two regions can arise if nucleation occurs earlier in some parts of the crystal than in others (e.g. due to possible temperature differences in different parts of the crystal during cooling) and in λ_1 and λ_2 if nucleation occurs at special sites which are not uniformly distributed in the crystal.

To summarize then, we can say that the precipitation of second phase particles and depletion of $C_a(t) - C_\infty$ in the Frank–Zener regime will be described by the equations given by Wert and Zener by one single relaxation time τ_z if all particles are of equal radii and if the distribution of particles is fairly uniform in the solid. Small fluctuations in λ or R will cause a distribution in the value of τ_z over a small range. However, if there are groups of nuclei or particles in high local concentrations, separated by a distance L such that $L \gg \lambda$, these groups will behave practically independently of each other. If $C_a(t)$ in any group is different from that in another group, the difference will persist for most of the precipitation period. In this case any measured macroscopic average of $C_a(t)$ will be a superposition of the values in the different regions. The application of this idea to precipitation data is discussed in more detail by Jain and Hughes [50].

3.5. LSW regime

Differentiating Equation 32 with respect to time and using Equation 31 we obtain

$$\frac{d(C_a - C_\infty)}{dt} = -\tfrac{1}{3}(C_a - C_\infty)/\tau_L \tag{46}$$

where

$$\tau_L = \frac{9R_c^3 C_p}{4\alpha D C_\infty} \tag{47}$$

is the characteristic time for the rate of change of $(C_a - C_\infty)$ in the LSW regime*. The distance over which any fluctuations will be smoothed out in this time is of order $(R_c^3 C_p/\alpha C_\infty)^{1/2}$. The condition for two different LSW systems in the same crystal to act independently thus becomes

$$L \gg \left(\frac{R_c^3 C_p}{\alpha C_\infty}\right)^{1/2} \tag{48}$$

where L is the distance between the two systems.

With $R_c/\alpha \sim 3$, $C_p/C_\infty \sim 10^3$ this gives

$$L/R_c \gg 50 \text{ i.e. } L/\lambda \gg 5 \text{ if } \lambda \sim 10R_c \tag{49}$$

as compared with Equation 45.

It should be noted that in neither the Frank–Zener regime nor the LSW regime is dC_a/dt properly linear in $(C_a - C_\infty)$, since, for example, τ_L is a function of time through R_c. Thus a comparison of the "time constants" τ_z or τ_L with L^2/D is only a very rough criterion. It would be more satisfactory to compare the value of dC_a/dt due to ripening within each LSW system with the rate at which the values of C_a in each region tend to change due to inter-region diffusion. We can express the latter approximately through

$$\left|\frac{d[C_a(2) - C_a(1)]}{dt}\right| \sim \frac{D}{L^2}[C_a(2) - C_a(1)]$$

$$= \frac{D\alpha C_\infty}{L^2}\left[\frac{1}{R_c(2)} - \frac{1}{R_c(1)}\right] \tag{50}$$

From Equations 46 and 47 we have, in terms of R_c

$$\left|\frac{dC_a(1)}{dt}\right| = \frac{4\alpha^2 C_\infty^2 D}{27 C_p R_c^4(1)} \tag{51}$$

Comparing Equations 50 and 51 we obtain the criterion for the two LSW regimes to be independent as

$$\frac{\alpha}{R_c^3(1)} \cdot \frac{C_\infty}{C_p} \gg \left|\frac{1}{L^2}\left[\frac{1}{\beta} - 1\right]\right| \tag{52}$$

with $R_c(2) = \beta R_c(1)$.

Equation 52 may be rewritten

$$L^2 \gg \left|\frac{R_c^3(1)}{\alpha}\frac{C_p}{C_\infty}\left[\frac{1}{\beta} - 1\right]\right| \tag{53}$$

which is essentially the same as Equation 48. If two LSW systems are to be recognized as ripening independently, $R_c(2)$ must be significantly different from $R_c(1)$ i.e. β appreciably greater or less than unity. Equation 53 shows that if $\beta \sim 0.5$ the condition for independent ripening is not difficult to satisfy. For example, even if $R_c \sim 20$ nm the two regions need only be separated by some μm in a typical case. In any given situation, one needs to examine the values of α, C_p and C_∞ relevant to the system concerned. However, we may conclude as a result of the arguments in this section that if groups of precipitates occur in an inhomogeneous distribution as a result of the nucleation process, they may subsequently undergo Ostwald ripening as almost independent LSW systems with different critical radii. Particle size distributions observed experimentally may therefore be superpositions of several different distribution functions of the types described in Section 2.

The arguments are quite easily extended to cover cases 1 and 3, with similar conclusions. In fact, the condition for independent ripening systems becomes easier to satisfy as one goes from case 1 through case 2 to case 3.

4. Comparison of the theory with experiments on non-metallic solids

4.1. Silver particles in glass

Kreibig [25] produced silver particles in photosensitive glass containing 0.02 to 0.06% of Ag_2O. Particles were nucleated by radiation from a mercury lamp or by X-rays. The particles were grown and ripened at 550° C. The glass was pulverized and dissolved in water and the size distribution of the particles thus released was measured using electron microscopy.

Efforts have been made to fit each of the theoretical curves [$F_1(u)$ for the surface reaction case, $F_2(u)$ for the bulk diffusion case and $F_3(u)$ for the dislocation diffusion case] with the size distribution measured by Kreibig. The fits were made by scaling the radius coordinate so that the peaks of the experimental histogram and the theoretical distributions come close together. Several such fits may be tried and their success judged by inspection. As shown in Fig. 4, $F_1(u)$ is too broad to give a satisfactory fit to the data. On the other hand, both the curves $F_2(u)$ and $F_3(u)$ are much too narrow when compared with the observed distribution. In any case one would not expect the dislocation or grain boundary case to be relevant for a glass.

*Note τ_L contains R_c^3 whereas τ_2 given in Section 2.3 contains $R_c^3(0)$, otherwise the expressions are similar.

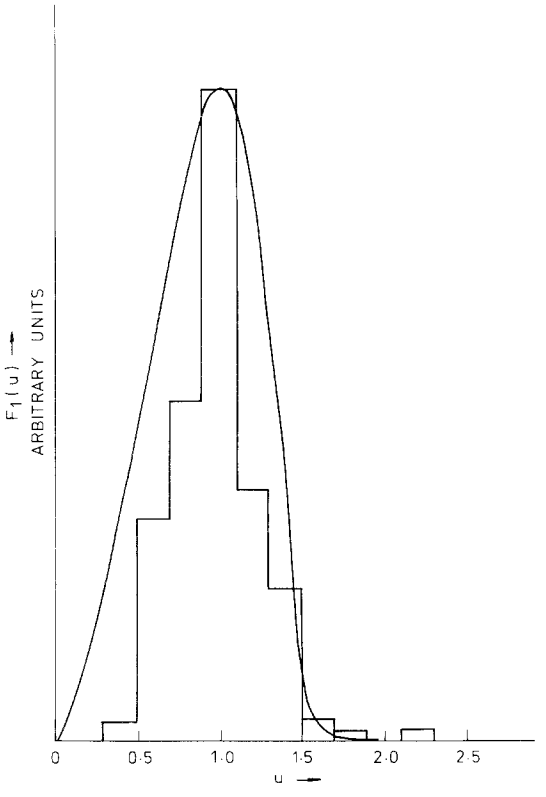

Figure 4 A comparison of the theoretical size distribution function $F_1(u)$ with the experimental data for silver particles in glass obtained by Kreibig [25]. The experimental data have been recast in terms of $u = R/R_c$ by choosing a value of R_c which gives the best visual fit.

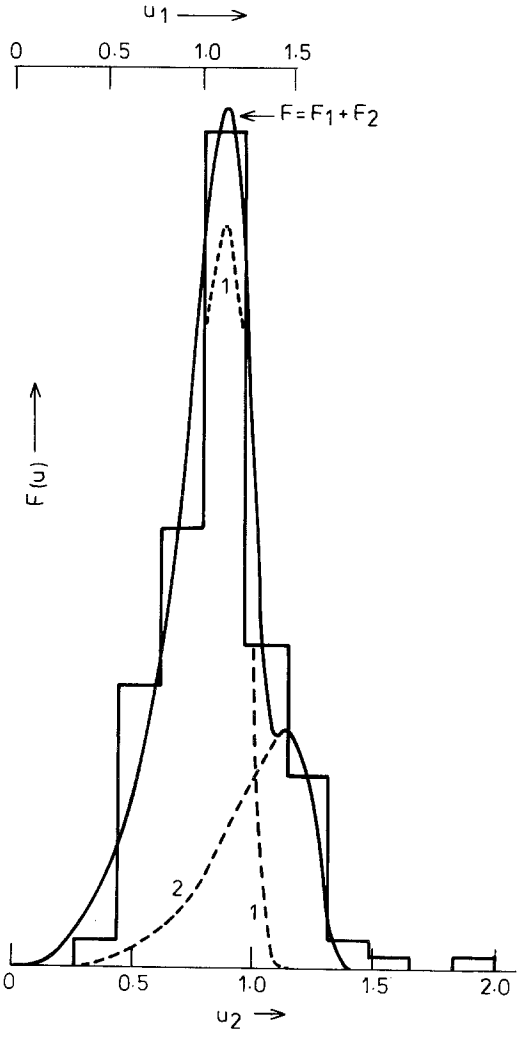

Figure 5 Evidence of two LSW systems of silver particles ripening independently in experiments made by Kreibig [25]. The observed size distribution, shown by histograms, fits with the composite curve $F = F_1 + F_2$, $F_1 = F_2(u_1)$ and $F_2 = F_2(u_2)$; the values of average radii for the two systems u_1 and u_2 are $\bar{R}_1 = 5.0\,\text{nm}$ and $\bar{R}_2 = 6.5\,\text{nm}$ respectively. Single LSW curves $F_1(u)$, $F_2(u)$ or $F_3(u)$ do not fit with the observations.

We suggested in Section 3 that all particles in a matrix need not necessarily form part of one LSW system. Based on this suggestion and the arguments given there, we have tried and fitted successfully two $F_2(u)$ curves with the observed distribution, the values of $\bar{R}$ being $\bar{R}_1 = 5.0\,\text{nm}$ and $\bar{R}_2 = 6.5\,\text{nm}$ for the two systems. It is seen from Fig. 5 that the curve $F = F_2(u_1) + F_2(u_2)$ ($u_1 = R/\bar{R}_1$ and $u_2 = R/\bar{R}_2$) agrees well with the observations.

Though this agreement of the sum of two $F_2(u)$ curves with observations supports strongly the suggestion that two or more LSW ripening groups occur independently in many cases, the real test of this suggestion would lie in the measurement of the interparticle distances and radius distributions in space in the sample. Unfortunately such information is not available in any of the size distribution measurements reported in the literature.

It is seen in Fig. 5 that there are a few very large particles ($R \sim 10$ to $13\,\text{nm}$) present in the system with a gap near $R \sim 11.5\,\text{nm}$ where there are no particles. We shall discuss briefly these large particles, along with the results of Shvarts *et al.* [24] and Chassagne *et al.* [29, 30], in Section 5.

4.2. Silver particles in KCl

Silver particles in alkali halides have been studied by several workers. Recently Jain and Arora [26] have measured the size distribution of the particles in KCl. The crystal was dissolved in water and the size of the particles thus released was measured with an electron microscope. The observed distributions for a crystal ripened for two different

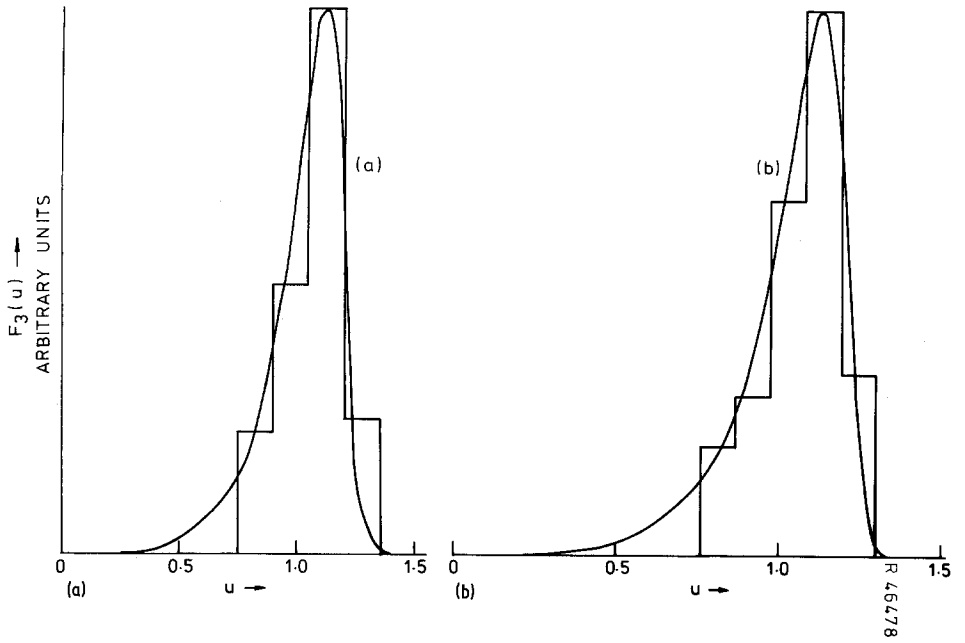

Figure 6 Ostwald ripening of silver particles in KCl by diffusion through dislocations observed by Jain and Arora [26]. The observed distributions (i.e. histograms) are perhaps the narrowest reported in the literature and can be fitted only with the sharp theoretical curves $F_3(u)$ obtained for ripening by diffusion though dislocations. (a) $2\bar{R} = 33$ nm and (b) $2\bar{R} = 46$ nm.

times are shown by the histograms in Figs. 6a and b respectively. The distributions are the narrowest of all the measured distributions on different systems we have seen so far (see for comparison the data given in [21] and references therein). The theoretical plot of $F_3(u)$, derived earlier (Section 2) for diffusion through dislocations, fits extremely well with the observations in both cases [51]. $F_2(u)$ is substantially too broad. Since the ripening was done at a rather high temperature (700° C), the result that the diffusion is almost completely controlled by transport through dislocations may appear surprising. However, the crystals were grown from the melt, quenched from high temperatures several times and contained a very high dislocation density. Durand *et al.* [38] have also found that metallic colloids are formed by migration of F-centres to dislocations even if the alkali halide crystals are not deformed. The most convincing evidence that the colloids are in fact formed at dislocations, even in undeformed crystals, is provided by the direct observations of colloids by Hobbs *et al.* [52] and Chassagne *et al.* [29, 30].

Calleja and Agulló-López [32] have attempted to fit these data for Ag colloids in KCl using the bulk diffusion distribution $F_2(u)$. They obtain an apparently good fit by superposing the two experimental distributions in Figs. 6a and b, assuming that the $t^{1/3}$ law holds for $\bar{R}$ ($\equiv R_c$). This superposition, however, results in a distribution which is substantially wider than each separate experimental histogram, and explains why they are able to get a good fit to $F_2(u)$. In fact the ripening times quoted by Jain and Arora [26] are not known precisely enough to test the time dependence of R_c, and the limited data fit neither $t^{1/3}$ nor $t^{1/4}$.

4.3. Suzuki phase in NaCl

Kirk *et al.* [27] have studied precipitates of the Suzuki phase $MnCl_2 \cdot 6NaCl$ in Mn doped NaCl crystals. The size distribution of the precipitates measured by them in a crystal containing 225 p.p.m. of $MnCl_2$ is shown in Fig. 7.

Although Mn diffusion is the rate-controlling process for the transport of Mn [27], a study of the Suzuki phase structure shows that both Mn^{2+} and its charge compensating cation vacancy have to be incorporated in the precipitate at specific locations. The Mn^{2+} ion and the cation vacancy do not form a nearest neighbour pair in the phase. It is not possible for the Mn^{2+} ion or the vacancy to attach themselves to the precipitate at the point of arrival on the surface of the precipitate. We therefore expect that a relatively slow surface reaction will control the growth kinetics and compare the

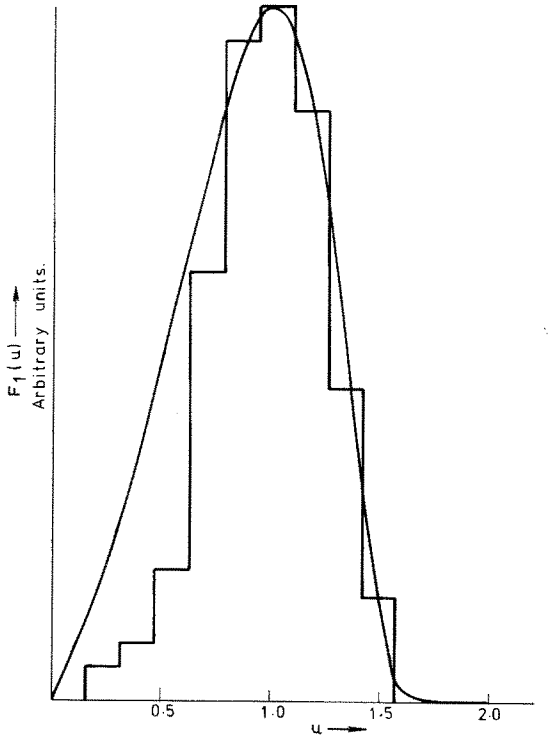

Figure 7 Size distribution of the Suzuki phase of $MnCl_2 \cdot 6NaCl$ cystals observed by Kirk, Kahn and Pratt [27] (histogram) and theoretical plot of $F_1(u)$, the LSW curve for surface controlled reaction for $\bar{R} = 128$ nm. The concentration of Mn in NaCl is 225 p.p.m. The small discrepancy between theory and experiment for $u < 0.5$ is probably not significant (see text). The cation vacancy and Mn^{2+} ion have to be incorporated in the precipitate at specific sites. Since they cannot deposit themselves onto the precipitates at the points of arrival, surface reaction is believed to be the rate-controlling mechanism.

theoretical distribution $F_1(u)$, Equation 26, with the experimental results in Fig. 7. The agreement of theory with experiment is good except for the very small number of particles for $u < 0.5$. This discrepancy is perhaps to be expected in view of the discussion of the approximation used in expanding Thomson's equation (Equation 13) in Section 3. It was mentioned earlier that this error is expected to be most apparent in the surface reaction case. $F_2(u)$ and $F_3(u)$ are much narrower than the experimental distribution, although it must be admitted that a superposition of several such curves would, of course, give a better fit.

5. The presence of large particles and the influence of gross inhomogeneities

We have seen in Section 4 that there were a few large particles of silver present in the glass in Kreibig's experiments. These did not form part of the two LSW systems which described the size distribution of the rest of the particles. The occurrence of these anomalously large particles is not unique to silver particles in glass and is found in many other systems. Chellman and Ardell [21] found such particles in metal alloys. Kirk *et al.* [27] also observed a few large precipitates of the Suzuki phase in their more heavily doped crystals of NaCl. The size distribution histograms of Kirk *et al.* became quite complex in the heavily doped crystals.

Shvarts *et al.* [24] have reported the size distribution of Na and K colloids in NaCl and KCl heavily coloured by electrolytic coloration. They found that the distribution of colloids was highly non-uniform in their crystals. A long tail on the large size side of the size distribution is observed in these crystals. The size distribution spectra of Chassagne *et al.* [29] are also very complex and show an anomalously large population of large particles. (Note that in the replica electron microscopy technique used by Shvarts *et al.*, the true size distribution is obtained from the measured size distribution by the method described by Lifshitz and Slezov [10]. This correction makes the true distribution of a slightly different shape from the observed one, but cannot explain the population of large particles or the tail on the large size side.)

A notable result of LSW theory for Ostwald ripening in all three cases considered is the sharp cut-off at some value of R close to but larger than $\bar{R}$ on the large size side. The presence of a few very large particles or a gradual tail on the large size side are results exactly opposite to the predictions of the theory.

The result derived in Section 3 that different groups of particles may form different LSW systems (or that there may be a more or less continuous distribution of $\bar{R}$) was based on a non-uniformity in the distribution of particles, but it was implicitly assumed that $\lambda \gg R$ (or $\lambda \gg a_e$ in the case of dislocations) for the particles in each system, so that the approximations of spherical symmetry and steady state diffusion are still valid. In any one LSW system, each particle "sees" all the other particles through its interaction with $C_a(t)$ (which is determined by the dR/dt of all particles). In this case, no single particle can go ahead and grow very large, as all particles with comparable radii $R > R_c$ draw the solute from $C_a(t)$ and grow at comparable rates.

A close study of the results of Shvarts *et al.* [24] and Chassagne *et al.* [29] shows that the distribu-

tion of particles in space in the crystals is characterized by large inhomogeneities. In many of the photographs of colloids in crystals [28–30], the spacing between the surfaces of the colloidal particles is less than the particle radii R. Chassagne *et al.* [29] also found that the number of F-centres lost during the ripening process was much larger than the number of alkali metal atoms present in the colloids obtained and measured with the help of the electron microscope. The discrepancy is very large and cannot be explained by taking into account the thermal diffusion of F-centres out of the crystal during the ripening process [31, 53, 54]. A more likely explanation [29] is that the inhomogeneous nature of the colloid distribution prevents the replication electron microscopy from providing a true average picture of the system. In both sets of experiments the colloid size distributions have complex shapes which change with annealing time. All these features suggest that in these systems we are dealing with conditions which result in at least some of the colloidal particles not meeting the criteria for forming an LSW system. In particular, it appears as if groups of particles are formed which have $\lambda \sim R$ instead of $\gg R$. These systems are very complex, since the concepts of steady state diffusion and spherical symmetry around each particle break down (see also Section 3.3). A satisfactory theory of Ostwald ripening under these conditions is not available (see however Chellman and Ardell [21] for a limited attempt at the problem). In addition, it is also possible that very closely spaced particles ($\lambda \sim R$) may coalesce by actual particle migration (driven in the case of colloids presumably by surface diffusion). This effect is not included in the main results of the LSW theory of ripening, but is extremely important for the growth of particles in gases and liquids where it is the dominant ripening process (see for example [55–61].

Despite these difficulties, we can understand in a general way the features of the size distribution for systems where some particles are formed very close together. Such a cluster of closely spaced particles can ripen independently of the behaviour of the rest of the particles in the solid (see Section 3.5), so that it may ripen relatively quickly into one large particle. If there are several such clusters of particles, after some period of ripening there will be a few very large particles originating from these clusters, plus the rest of the solid which may still contain one or more groups of more dispersed particles which are still forming LSW systems. In any one experiment, the particle size distribution is then likely to display evidence for an LSW-type distribution plus some "anomalously" large particles.

6. Conclusions

In this paper we have examined the basic Lifshitz–Slezov–Wagner theory of Ostwald ripening, extended it to include diffusion of solute along dislocations or grain boundaries, and explored the conditions under which it may be expected to hold in practice. It is apparent from this study that it is quite possible for different regions of the same solid to ripen independently. This behaviour seems to be borne out when attempts are made to apply the simple theory to the growth of particles in ionic crystals, since several of the systems studied show features which cannot be explained on the basis of one ripening system. In particular, some very large particles are often found which are very likely to have resulted from special regions where a few closely spaced particles have relatively quickly ripened or coalesced into one precipitate. This possibility is consistent with the very inhomogeneous distributions of particles observed by electron microscopy.

One characteristic of the systems to which we have applied the theory is that they are generally rather dilute by comparison with precipitation problems which have been studied in alloys. For example, the total "solute" concentration in the case of the growth of colloids from F-centres in alkali halides is $<0.1\%$, whereas in metallurgical applications of LSW theory to the coarsening of Ni_3Al particles in Ni–Al alloys the solute concentration may be several percent. Nevertheless, some of the discrepancies between LSW theory and observations in metallurgical systems may, on careful examination, be due to some of the limitations of the theory which we have discussed.

Appendix 1

List of symbols used

σ	interfacial energy (ergs cm^{-2})
α	$2\sigma\Omega/kT$ (cm)
Ω	atomic volume of solute atom (cm^3)
λ	interparticle separation (cm)
R	radius of the particle (cm)
R_c	critical radius
$R_c(0)$	value of R_c at $t = 0$

$\bar{R}$	average radius
u	reduced radius R/R_c
K	surface reaction rate constant (cm sec^{-1})
D	bulk diffusion coefficient (cm^2 sec^{-1})
D_l	dislocation diffusion coefficient
D_g	grain boundary diffusion coefficient
G	rate constant in dislocation or grain boundary case (cm^3 sec^{-1})
C	solute concentration at general point (cm^{-3})
C_R	solute concentration at surface of precipitate of radius R
C_a	average concentration of solute in bulk of crystal
C_∞	concentration of solute in equilibrium with a plane surface ($R \to \infty$)
C_p	concentration of solute atoms in the particle
t	time (sec)
τ	relaxation time
$n(t)$	number density of particles at time t (cm^{-3})
a	radius of dislocation line (cm)
a_e	effective value of a
b	thickness or width of grain boundary (cm)
s	perpendicular distance from the core of a dislocation line or from a grain boundary
x	distance from the centre of the particle along the dislocation line or in the grain boundary plane
j	solute current into particle
$j(x)$	solute current from bulk into the dislocation line (or grain boundary,) cm^{-1} (or cm^{-2}) sec^{-1}
B	strength of potential of the dislocation stress field
L	separation of two regions of crystal.

Appendix 2
Rate of change of particle radius due to dislocation and grain boundary diffusion of solute atoms

In the steady state approximation where $\partial C/\partial t = 0$ at all points in the solid, a number of different approaches can be used to calculate dR/dt for dislocation or grain boundary diffusion. We consider these in this appendix. In all cases, we shall neglect the influence of the particle itself on the diffusion process to or along the dislocation or grain boundary, so that the diffusion problem retains the symmetry of the line or planar defect. This approximation will be reasonable provided the particle radius R is much smaller than the interparticle separation λ or, more precisely, smaller than the distance over which the solute concentration achieves its mean bulk value C_a.

1. Dislocation diffusion

The geometry of the problem is shown in Fig. 1a.

(a) Let us assume first of all that there is no appreciable diffusion of solute from the bulk to the dislocation line, but that the solute concentration in the dislocation is maintained at the bulk value C_a at a distance $x = d$ ($d \gg R$) from the particle by some means.

In the steady state

$$D_l \frac{\partial^2 C(x)}{\partial x^2} = 0 \qquad \text{(A1)}$$

so that with boundary conditions $C(x) = C_R$ at $x = R$ and $C(x) = C_a$ at $x = d$ we find that the current density j of solute *into* the particle is given by

$$j = D_l \left(\frac{\partial C(x)}{\partial x} \right)_{x=R} = \frac{D_l}{d}(C_a - C_R) \qquad \text{(A2)}$$

(b) Suppose now that there is lateral diffusion of solute into the dislocation from the bulk. In the steady state the equation of continuity is then*

$$\pi a^2 D_l \frac{\partial^2 C(x)}{\partial x^2} + j(x) = 0 \qquad \text{(A3)}$$

where

$$j(x) = 2\pi a D \left(\frac{\partial C(s)}{\partial s} \right)_{s=a} \qquad \text{(A4)}$$

*This treatment does not explicitly include the drift of solute into the dislocation by virtue of the elastic interaction between the dislocation and a solute atom. This may be included in a crude way by an appropriate choice of the distance a as the interaction distance. (See Equation 6).

To find $j(x)$ we need $C(s)$, which can be found in the steady state approximation since in cylindrical symmetry

$$\frac{1}{s}\frac{\partial}{\partial s}\, s\,\frac{\partial C(s)}{\partial s} = 0 \qquad \text{(A5)}$$

This gives, with boundary conditions $C(s) = C(x)$ at $s = a$ and $C(s) = C_a$ at $s = l$

$$C(s) = C_a + \frac{[C_a - C(x)]\ln(s/l)}{\ln(l/a)} \qquad \text{(A6)}$$

so that

$$j(x) = \frac{2\pi D[C_a - C(x)]}{\ln(l/a)} \qquad \text{(A7)}$$

Substituting this in Equation A3 and putting $C(x) - C_a = y$, we find

$$\frac{\partial^2 y}{\partial x^2} - K^2 y = 0 \qquad \text{(A8)}$$

where

$$K^2 = \frac{2D}{a^2 D_1 \ln(l/a)} \qquad \text{(A9)}$$

Thus $y = Ae^{-Kx} + Be^{Kx}$ where A and B are found from the boundary conditions

$$y = C_R - C_a \text{ at } x = R$$
$$y = 0 \text{ at } x = d(d \to \infty)$$

This leads to a current density into the particle given by

$$j = D_1\left(\frac{\partial C(x)}{\partial x}\right)_{x=R} \qquad \text{(A10)}$$
$$= D_1 K[C_a - C_R]\coth[K(d-R)]$$

If $D \to 0, K \to 0$ and $\coth[K(d-R)] \simeq 1/K(d-R)$, so that Equation A10 reduces to Equation A2 as expected. If $d \to \infty$ for finite K then

$$j = D_1 K(C_a - C_R) \qquad \text{(A11)}$$

(c) An alternative approximation is to assume that the solute in the dislocation pipe behaves like a "gas" with constant concentration C_R. The current into the particle must then equal the total lateral flow into the dislocation
i.e.

$$\pi a^2 j = \int_R^d j(x)dx \quad (d \gg R) \qquad \text{(A12)}$$

with

$$j(x) = \frac{2\pi D}{\ln(l/a)}(C_a - C_R)$$

Thus

$$j \simeq \frac{2Dd}{a^2 \ln(l/a)}(C_a - C_R) \qquad \text{(A13)}$$

This is essentially the "gas-like" model of Bullough and Newman [36]. The rate of change of particle radius is given by*

$$(C_p - C_R)\,4\pi R^2\,dR/dt = 2\pi a^2 j$$

So that in all cases we have

$$\frac{dR}{dt} = \frac{G}{R^2}\frac{(C_a - C_R)}{C_p} \quad (C_p \gg C_R)$$

where: case (a) $G = a^2 D_1/2d$

case (b) $G = \frac{a}{2}\sqrt{\left(\frac{2DD_1}{\ln(l/a)}\right)}\ (d \to \infty)$

case (c) $G = \frac{Dd}{\ln(l/a)}$

Thus the form of dR/dt is independent of which model is used, although the interpretation of the factor G differs for the three cases.

2. Grain boundary diffusion

The geometry of the problem is shown in Fig. 1b.

(a) If there is no transport from the bulk to the grain boundary then in the boundary plane we have, in the steady state

$$\frac{1}{x}\frac{\partial}{\partial x}\, x\,\frac{\partial C(x)}{\partial x} = 0. \qquad \text{(A14)}$$

This gives (c.f. Equations A5 to A7) the current density into the particle as:

$$j = D_g\left(\frac{\partial C(x)}{\partial x}\right)_{x=R} = D_g\frac{(C_a - C_R)}{R\ln(d/R)} \qquad \text{(A15)}$$

where $C(x) = C_a$ at $x = d(\gg R)$.

*A single dislocation pipe cuts the particle over an area πa^2 on each side. The extension to more than one dislocation is obvious.

(b) If there is lateral diffusion from the bulk to the grain boundary then the equation of continuity is

$$\frac{b}{x} D_g \frac{\partial}{\partial x} x \frac{\partial C(x)}{\partial x} + j(x) = 0 \qquad \text{(A16)}$$

where

$$j(x) = 2D\left(\frac{\partial C(s)}{\partial s}\right)_{s=b/2} \qquad \text{(A17)}$$

(The 2 occurs because solute enters from both sides.)

To find $j(x)$ we use the fact that the lateral problem is a one-dimensional one so that

$$\left(\frac{\partial C(s)}{\partial s}\right)_{s=b/2} = \frac{C_a - C(x)}{l - b/2} \qquad \text{(A18)}$$

where

$$C(s) = C_a \text{ at } s = l.$$

Thus Equation A16 becomes, with $C(x) - C_a = y$

$$\frac{1}{x}\frac{\partial}{\partial x} x \frac{\partial y}{\partial x} - K'^2 y = 0 \qquad \text{(A19)}$$

where

$$K'^2 = \frac{2D}{D_g b(l - b/2)} \qquad \text{(A20)}$$

If we now put $K'x = z$, Equation A20 can be converted to

$$z \frac{\partial}{\partial z} z \frac{\partial y}{\partial z} - z^2 y = 0 \qquad \text{(A21)}$$

which is Bessel's equation with $n = 0$ (see [62], Chapter 21).

We seek a solution to this equation which tends to zero as z tends to infinity ($C(x) \to C_a$ as $x \to \infty$), so that we choose the zeroth order Bessel function $K_0(z)$ ($K_0(z) \to e^{-z}\sqrt{(2/\pi z)}$ as $z \to \infty$ (see [62], p. 584 where the functions $K_n(z)$ are denoted by $Kh_n(z)$).

Thus we have $y = AK_0(z)$, with the constant of integration A determined by the boundary condition $y = C_R - C_a$ when $z = K'R$ i.e.

$$A = (C_R - C_a)/K_0(K'R).$$

The current dentsity of solute atoms into the particle is then

$$j = D_g\left(\frac{\partial C(x)}{\partial x}\right)_{x=R}.$$

Since $\frac{d}{dz}[K_0(z)] = -K_1(z)$ we have

$$j = D_g K'(C_a - C_R)\frac{K_1(K'R)}{K_0(K'R)} \qquad \text{(A22)}$$

To proceed further, we note that for large values of x the solution $y = C(x) - C_a$ varies as

$$C(x) - C_a \simeq \sqrt{\left(\frac{2}{\pi}\right)}\frac{e^{-K'x}}{\sqrt{(K'x)}}. \qquad \text{(A23)}$$

Since the approximations we have made require the particle of radius R to be much smaller than the distance over which $C(x)$ varies significantly, which is of order $x \sim 1/K'$, we must have $R \ll 1/K'$ i.e. $K'R \ll 1$ or $D_g/D \gg R^2/lb$. We can than use the small z approximations for the Bessel functions, which lead to ([62], p. 580)

$$K_0(z) \simeq -\frac{2}{\pi}\ln(z/2) \qquad \text{(A24)}$$

$$K_1(z) \simeq \frac{2}{\pi}(1/z) \qquad \text{(A25)}$$

so that

$$j = \frac{D_g(C_a - C_R)}{R \ln(2/K'R)} \qquad \text{(A26)}$$

This is identical to Equation A15 if $2/K' \equiv d$.

(c) In the "gas-like" approximation (c.f. case (c) of the dislocation problem) we assume that $C(x) \equiv C_R$ and

$$2\pi Rbj = \int_R^d 2\pi x j(x)dx \simeq \frac{\pi d^2 2D(C_a - C_R)}{l - b/2} \qquad \text{(A27)}$$

Thus

$$j = \frac{Dd^2(C_a - C_R)}{b(l - b/2)R} \qquad \text{(A28)}$$

Assuming a spherical particle (see Greenwood [20] for the different numerical constants appropriate to a particle of a shape which is in equilibrium with the grain boundary forces) the rate of change of particle radius is

$$(C_p - C_R)\,4\pi R^2\,(dR/dt) = 2\pi Rbj.$$

In all three cases we therefore have

$$\frac{dR}{dt} = \frac{G}{R^2}\frac{(C_a - C_R)}{C_p} \quad (C_p \gg C_R)$$

where: case (a) $G = \dfrac{D_g b}{2 \ln (d/R)}$

case (b) $G = \dfrac{D_g b}{2 \ln (2/K'R)}$

case (c) $G = \dfrac{Dd^2}{2(l - b/2)}$

Case (a) is essentially the same as that used by Greenwood [20] and Chakraverty [41]. Since $\ln (d/R)$ and $\ln (2/K'R)$ are very slowly varying functions of $R(\ll d, \ll 2/K')$, G is sensibly constant in all three cases.

Thus we conclude that, with these approximations, both dislocation and grain boundary diffusion lead to expressions for dR/dt of the same general form in which $dR/dt \propto R^{-2}$. This should be compared with bulk diffusion in which case $dR/dt \propto R^{-1}$.

Appendix 3

Derivation of size distribution for the dislocation or grain boundary diffusion case

The expression derived in Appendix 2 for the rate of change of particle radius is

$$\frac{dR}{dt} = \frac{G}{R^2} \frac{(C_a - C_R)}{C_p} \tag{A29}$$

Using $(C_R - C_\infty)/C_\infty = \alpha/R$ and $(C_a - C_\infty)/C_\infty = \alpha/R_c$ this becomes

$$\frac{dR}{dt} = \frac{G\alpha C_\infty}{C_p R^2} \left(\frac{1}{R_c} - \frac{1}{R} \right) \tag{A30}$$

Making substitutions to dimensionless variables $\rho = R/R_c(0), x = R_c/R_c(0)$ and

$$t' = t \left(\frac{\alpha G C_\infty}{C_p R_c^4(0)} \right)$$

Equation A30 becomes

$$\frac{d\rho}{dt'} = \frac{1}{\rho^3} (\rho/x - 1) \tag{A31}$$

which is similar to the equation obtained by Lifshitz and Slezov for the bulk diffusion case, except that theirs has $1/\rho^2$ on the right hand side instead of $1/\rho^3$.

We now follow the Lifshitz and Slezov procedure and change to variables*

$$u = \rho/x = R/R_c \tag{A32}$$

$$\tau = \ln (x^4) \tag{A33}$$

This procedure is followed so as to replace the time variable t' with the variable τ, which measures time since the critical radius variable x will increase monotonically with time as the solute supersaturation $(C_a - C_\infty)$ decreases†. Equation A31 can then be transformed to

$$\frac{du^4}{d\tau} = \gamma(\tau)(u - 1) - u^4 \tag{A34}$$

where

$$\gamma(\tau) = 4 \frac{dt'}{d(x^4)} \tag{A35}$$

Note that the presence of x^4 in Equation A35 is unrelated to the use of x^4 in Equation A35, but originates in the fact that Equation A33 has ρ^3 in the denominator. In terms of the original variables:

$$\gamma(\tau) = \frac{4\alpha G C_\infty}{C_p} \frac{dt}{d(R_c^4)} \tag{A36}$$

which brings out the way γ depends on the time variation of R_c.

Lifshitz and Slezov argue that $\gamma(\tau)$ will tend asymptotically to a constant for large τ, and furthermore that the value of this constant is such as to make both $du/d\tau$ and its first derivative with respect to u zero at some point $u = u_0$. The arguments of Lifshitz and Slezov are quite general and are applicable to the surface reaction case discussed by Wagner [13] and to this case (irrespective of the highest power of u in Equation A34). Using this same prescription in our case leads to

$$u_0 = 4/3 \tag{A37}$$

and

$$\gamma_0 = 4u_0^3. \tag{A38}$$

Thus we find

$$g(u) = -\frac{du}{d\tau} = \frac{u^4 - 4u_0^3 (u - 1)}{4u^3} \tag{A39}$$

*Note that the power of x used in τ is arbitrary, and does not influence the final results. We choose x^4 to make a parallel with the Lifshitz and Slezov use of x^3 in the bulk diffusion case.

†This holds provided the particles are not initially all of exactly the same size, see Lifshitz and Slezov [10].

The problem is now to use Equation A39 to derive a size distribution function $f(R, t)$ where $f(R, t)$ is the number density of particles with radius in the range R to $R + dR$ at time t. In terms of the new variables ρ and u we can derive two new distribution functions $F(\rho)$ and $\phi(u)$ such that

$$f(R, t)dR = F(\rho, t)d\rho = \phi(u, \tau)du. \quad \text{(A40)}$$

Thus

$$\phi(u, \tau) = R_c f(R, t) \quad \text{(A41)}$$

$$F(\rho, t) = R_c(0) f(R, t). \quad \text{(A42)}$$

These distribution functions must satisfy two constraints.

(a) The continuity equation

$$\frac{\partial}{\partial t} f(R, t) + \frac{\partial}{\partial R}[f(R, t)\dot{R}] = 0 \quad \text{(A43)}$$

which in u, τ space becomes

$$\frac{\partial \phi(u, \tau)}{\partial \tau} - \frac{\partial}{\partial u}[\phi(u, \tau) g(u)] = 0 \quad \text{(A44)}$$

(since from Equation A39 $du/d\tau = -g(u)$).

(b) The conservation of total number of solute atoms per unit volume, N_0, which in terms of the initial relative supersaturation defined by $Q_0 = (N_0 - C_\infty)/C_p$ becomes

$$Q_0 = \frac{C_a - C_\infty}{C_p} + \frac{4\pi}{3} \int_0^\infty f(R, t) R^3 dR \quad \text{(A45)}$$

With some manipulation this can be converted to

$$1 = \frac{\alpha}{R_c(0) Q_0} \frac{C_\infty}{C_p} \frac{1}{x} + K \int_0^\infty F(\rho, t) \rho^3 d\rho \quad \text{(A46)}$$

or

$$1 = \frac{\alpha}{R_c(0) Q_0} \frac{C_\infty}{C_p} e^{-\tau/4} + K e^{3\tau/4} \int_0^\infty \phi(u, \tau) u^3 du$$

where

$$K = \frac{4\pi R_c^3(0)}{3 Q_0} \quad \text{(A47)}$$

Using a slight variant on the Lifshitz and Slezov approach, we note that if Equation A47 is to be satisfied as $\tau \to \infty$, $\phi(u, \tau)$ must have the form

$$\phi(u, \tau) = \text{constant } e^{-3\tau/4} F_3(u) \quad \text{(A48)}$$

Substituting Equation A48 into the continuity equation A44 we then find an expression for $F_3(u)$

$$-\ln F_3(u) = \frac{3}{4} \int \frac{du}{g(u)} + \ln g(u) + \text{constant} \quad \text{(A49)}$$

so that $F_3(u)$ can be deduced with the aid of Equation A39

To perform the integration of $1/g(u)$ we note that, using $u_0 = 4/3$, it can be transformed to

$$\frac{1}{4g(u)} = \frac{u^3}{(u - u_0)^2 [(u + u_0)^2 + 2u_0^2]} \quad \text{(A50)}$$

$$= \frac{(11/18)u + (2/3)u_0}{u^2 + 3u_0^2 + 2uu_0} + \frac{7/18}{u - u_0} + \frac{(1/6)u_0}{(u - u_0)^2} \quad \text{(A51)}$$

After some manipulation to perform the integrals, we obtain

$$F_3(u) = \frac{\text{constant } u^3 \exp\left[\frac{-2}{3(u_0 - u)}\right] \exp\left[-\frac{1}{6\sqrt{2}} \tan^{-1}\left(\frac{u + u_0}{u_0\sqrt{2}}\right)\right]}{(u_0 - u^{19/6})(u^2 + 2u_0 u + 4u_0)^{23/12}}$$

$$\text{for } u \leqslant u_0 = 4/3$$

$$F_3(u) = 0 \text{ for } u > u_0 \quad \text{(A52)}$$

This distribution is shown in Fig. 2. The mean value of u is $\bar{u} \simeq 1$ so that $\bar{R} \simeq R_c$. In fact it can be shown by differentiating Equation A45 with respect to time and assuming that $f(R, t)$ and C_a are slowly varying functions of time that

$$\int_0^\infty f(R, t) R^2 \left(\frac{dR}{dt}\right) dR \approx 0$$

which with the aid of Equation A30 for dR/dt gives $R_c^{-1} = \bar{R}^{-1}$. This procedure is an extension of the method used by Wagner [13] for the surface reaction and bulk diffusion limited cases. The approximations used are equivalent to taking the asymptotic solutions of Lifshitz and Slezov, which are valid for $x = R_c/R_c(0) \gg 1$ i.e. large τ.

Since we have assumed that $\gamma(\tau) \to$ constant $= 4u_0^3$ we also have

$$R_c^4 = R_c^4(0)(1 + t/\tau_3) \quad \text{(A53)}$$

where

$$\tau_3 = \frac{64 C_p R_c^4(0)}{27 \alpha G C_\infty} \qquad \text{(A54)}$$

The supersaturation $(C_a - C_\infty) \propto 1/R_c$ therefore falls like $t^{-1/4}$.

The number of particles per unit volume $n(t)$ is, at long times $t \gg \tau_3$

$$n(t) = \int_0^\infty \phi(u, \tau) du = \text{constant } e^{-3\tau/4} \propto t^{-3/4} \qquad \text{(A55)}$$

Finally using Equation A41

$$f(R, t) = \frac{\text{constant}}{t^{3/4}} \frac{F_3(R/R_c)}{R_c}$$

$$= \frac{\text{constant}}{t} F_3(R/R_c). \qquad \text{(A56)}$$

Acknowledgements

We should like to thank Drs L. W. Hobbs, A. B. Lidiard, A. D. LeClaire and R. Bullough for many discussions and helpful comments. The material in this review was originally produced as an AERE report, R8415. We are grateful to the Reviews Editor, Professor G. D. Sims, for his advice on converting the report into this article.

References

1. F. C. FRANK, *Proc. Roy. Soc.* **A201** (1950) 586.
2. C. ZENER, *J. Appl. Phys.* **20** (1949) 950.
3. C. WERT, *ibid.* **20** (1949) 943.
4. C. WERT and C. ZENER, *Phys. Rev.* **76** (1949) 1169.
5. *Idem, J. Appl. Phys,* **21** (1950) 5.
6. F. S. HAM, *J. Phys. Chem. Solids* **6** (1958) 335.
7. *Idem, J. Appl. Phys.* **30** (1959) 915.
8. J. W. CHRISTIAN, "The Theory of Transformations in Metals and Alloys" 2nd edn (Pergamon Press, Oxford, 1975).
9. G. W. GREENWOOD, *Acta Met.* **4** (1956) 243.
10. I. M. LIFSHITZ and V. V. SLEZOV, *J. Exptl. Theoret. Phys. (USSR)* **35** (1958) 479. (English Translation, *Soviet Phys JETP* **35** (1959) 311).
11. *Idem, Fiz Tverd Tela* **1** (1959) 1401 (English Translation, *Sov. Phys. Sol. Stat.* **1** (1959) 1285).
12. *Idem, J. Phys. Chem. Solids* **19** (1961) 35.
13. C. WAGNER, *Z. Elektrochem* **65** (1961) 581.
14. A. J. ARDELL, *Acta Met* **20** (1972) 61.
15. W. J. DUNNING, "Particle Growth in Suspensions," edited by A. L. Smith (Academic Press, London, 1973) p. 3.
16. M. KAHLWEIT, *Ber. Bunsen Gesell für Phys. Chemie.* 78 (1974) 997.
17. *Idem, Adv. Colloid and Interface Sci.* **5** (1975) 1.
18. *Idem, Scripta Met.* **10** (1976) 601.
19. *Idem, "Physical Chemistry: an Advanced Treatise"*, Vol. 10, Edited by H. Eyring, D. Henderson and W. Jost (Academic Press, New York, 1970) Chapter 11.
20. G. W. GREENWOOD, "The Mechanism of Phase Transformations in Crystalline Solids", Institute of Metals Monograph No. 33 (1969) p. 103.
21. D. J. CHELLMAN and A. J. ARDELL, *Acta Met,* **22** (1974) 577.
22. A. F. SMITH, *ibid* **15** (1967) 1867.
23. T. MUKHERJEE and C. M. SELLARS, "The Mechanism of Phase Transformations in Crystalline Solids," Institute of Metals Monograph, No. 33 (1969) p.122.
24. K. K. SHVARTS, Yu. A. EKMANIS, V. V. UDOD, A. F. LYUSHINA, Yu. E. TILIKS and R. A. Kan, *Fiz. Tver. Tela* **12** (1970) 879; (English Translation *Sov. Phys. Sol. Stat.* **12** (1970) 679).
25. U. KREIBIG, *J. Phys. F* **4** (1974) 999.
26. S. C. JAIN and N. D. ARORA, *J. Phys. Chem. Solids.* **35** (1974) 1231.
27. D. L. KIRK, A. R. KAHN and P. L. PRATT, *J. Phys. D* **8** (1975) 2013.
28. G. CHASSAGNE, Thesis, Université Claude Bernard, Villeurbanne, France (1976).
29. G. CHASSAGNE, D. DURAND, J. SERUGHETTI and L. W. HOBBS, *Phys. Stat. Sol.* **(a) 40** (1977) 629.
30. *Idem, ibid* **(a) 41** (1977) 183.
31. J. M. CALLEJA and F. AGULLÓ-LÓPEZ, *ibid* **(a) 25** (1974) 473.
32. *Idem, Phys. Lett.* **53A** (1975) 317.
33. A. D. BRAILSFORD and H. B. AARON, *J. Appl. Phys.* **40** (1969) 1702.
34. M. V. SPEIGHT, *Acta Met* **16** (1968) 133.
35. R. V. DAY and J. BARFORD, *Nature* **217** (1968) 1145.
36. R. BULLOUGH and R. C. NEWMAN, *Reports on Progress in Phys.* **33** (1970) 101.
37. H. I. AARONSON, H. B. AARON and K. R. KINSMAN, *Metallography* **4** (1971) 1.
38. D. DURAND, G. CHASSAGNE and J. SERUGHETTI, *Phys. Stat. Sol.* **(a) 12** (1972) 389.
39. A. H. COTTRELL and B. A. BILBY, *Proc. Phys. Soc. London* **A62** (1949) 49.
40. H. S. CARSLAW and J. C. JAEGER, "Conduction of Heat in Solids," 2nd edn (Oxford University Press. 1959) p. 189.
41. B. K. CHAKRAVERTY, *J. Phys. Chem. Sol.* **28** (1967) 2401.
42. R. D. VENGRENOVITCH and V. I. PSAREV, "Dispersed Metal Films" (in Russian) (Inst. Fiz. AN Ukr SSR, Kiev, 1972) p. 62.
43. R. D. VENGRENOVITCH, *Izv. Vuz. Fiz.* **3** (1974) 118 (English Translation, *Sov. Phys. J.* (USA) **3** (1974) 387).
44. R. A. ORIANI, *Acta Met.* **12** (1964) 1399.
45. C-Y. LI, J. M. BLAKELY and A. H. FEINGOLD, *ibid,* **14** (1966) 1397.
46. A. B. SCOTT, *Phil. Mag.* **45** (1954) 610.
47. J. G. FRIPIAT, K. T. CHOW, M. BOUDART, J. B. DIAMOND and K. H. JOHNSON, *J. Mol. Catalysis,* **1** (1975/76) 59.

48. R. F. MARSHALL, R. J. BLINT and A. B. KUNZ, *Sol. Stat. Comm.* **18** (1976) 731.
49. H. B. AARON, D. FAINSTEIN and G. R. KOTLER, *J. Appl. Phys.* **41** (1970) 4404.
50. S. C. JAIN and A. E. HUGHES, *Proc. Roy. Soc.* **A360** (1978) 47.
51. A. E. HUGHES and S. C. JAIN, *Phys. Lett.* **58A** (1976) 61.
52. L. W. HOBBS, A. E. HUGHES and G. CHASSAGNE, *Nature* **252** (1974) 383.
53. S. C. JAIN and G. D. SOOTHA, *Phys. Rev.* **171** (1968) 1075.
54. S. C. JAIN and V. K. JAIN, *ibid.* **181** (1969) 1312.
55. M. SMOLUCHOWSKI, *Physik. Z* **17** (1916) 557, 585.
56. *Idem, Z. Physik. Chem.* **92** (1917) 129
57. S. CHANDRASEKAR, *Rev. Mod. Phys.* **15** (1943) 1.
58. G. M. HIDY, *J. Colloid Sci.* **20** (1965) 123.
59. D. L. SWIFT and S. K. FRIEDLANDER, *ibid* **19** (1964) 621.
60. R. L. ROWELL and A. B. LEVIT, *J. Colloid Interface Sci.* **34** (1970) 585.
61. Y. E. GEGUZIN and M. A. KRIVOGLAZ, "Migration of Macroscopic Inclusions in Solids" (Consultants Bureau, New York and London, 1973).
62. H. JEFFREYS and B. S. JEFFREYS, "Methods of Mathematical Physics," 3rd edn (Cambridge University Press, 1966).

Received 1 October and accepted 18 October 1977.